Chapter III

Nitrogenase MoFe Protein from *Clostridium pasteurianum* at 1.08 Å Resolution: Comparison to the *Azotobacter vinelandii* MoFe Protein

This chapter summarizes my contributions to the publication of the same title written by Prof. Limei Zhang.[64] doi: 10.1107/S1399004714025243.

III.A. Abstract

The MoFe protein from *Azotobacter vinelandii* (Av1) is the most heavily studied nitrogenase protein for its structural and spectroscopic properties. Herein, we report the structural characterization of the most structurally divergent MoFe protein known, that from *Clostridium pasteurianum* (Cp1). The Cp1 structure was published in 1992 for the first (and, until this work, only) time with a resolution of 3.0 Å.[65] While this was useful for comparisons of the secondary protein structure, a detailed comparison of atomic positions, especially at the cofactors, could not be made. This work includes detailed comparisons of Av1 and Cp1, with an emphasis on the Fe protein docking site on the MoFe protein, the identity of the interstitial atom, and the P-cluster binding pocket. The results show that the structure of the cofactors is strictly conserved between Av1 and Cp1 homologs; however, differences in the secondary structure at the Fe protein docking site and in the P-cluster binding pocket may suggest some variation in the function of Av1 and Cp1.

III.B. Introduction

There are dozens of bacterial species that express nitrogenase; they are identified by the presence of nitrogen-fixing, "nif", genes in their genome.[24] Based on sequence alignment, these nitrogenases have been divided into six groups.[24] The two major groups are those with sequences similar to *Azotobacter vinelandii* (Av, group I) and *Clostridium pasteurianum* (Cp, group II). Groups III and IV are similar to Av but have small insertions or deletions; groups V and VI are nitrogenases that contain Fe or V in the FeMo-cofactor instead of Mo. The vast majority of nitrogenase work is performed using Av proteins.[19,22,28,37,38] By identifying similarities and differences between the MoFe proteins in different groups, we may further our understanding of the biological nitrogen fixation mechanism. Prior to this study, the only structure of a MoFe protein not from group I was the MoFe protein from Cp (Cp1) at 3.00 Å (PDB ID 1MIO).[21] This was a major accomplishment in understanding the greater structural differences between group I and II homologs; however, the resolution was too low to make definitive conclusions on atomic positions or the structure of the FeMo-cofactor. In this work, we report a high resolution structure of Cp1 and compare it to the high resolution structure of Av1 (PDB ID 3U7Q).[22]

III.B. Results

The published Cp1 structure, PDB ID 4WES, was solved to 1.08 Å resolution.[64] I used a dataset from a different crystal to create a structure solved to 1.12 Å resolution. The 1.12-Å Cp1 structure was determined by experimental phasing from multi-wavelength anomalous diffraction (MAD) data. Data processing and refinement statistics are provided in Table III-1. 10 of the 11 outliers in the Ramachandran plot include α-Ile48, α-Ser181, α-Gly345, α-Ser346, and α-Ala463, all of which are found in the interior of the protein and have well-defined electron density. These residues are not conserved in Av1, and may therefore be a characteristic of Cp1.

Four residues in the Cp1 structure have a peptide angle significantly distorted from 180°: α-Leu240 (~6°), α-Gly488 (~10°), β-Phe201 (~339°), and β-Phe411 (~351°). None of these residues are in areas of the protein identified as mechanistically important. The latter three exist in loop regions and are followed by a proline. α-Leu240 occurs between two threonine residues, the three of which make up the terminal strand of a beta sheet. α-Leu240 and α-Thr241 make a non-proline *cis*-peptide bond; this is the only non-proline *cis*-peptide bond observed in the MoFe protein.[22,66] In group I, the *cis*-peptide residues (α-Trp253 and α-Ser254 in Av1) are conserved 87%; those in group II (α-Leu240 and α-Thr241 in Cp1) are conserved 39%, indicating that the *cis*-peptide is more conserved among the Av1 homologs than the Cp1 homologs.

Table III-1. Data processing and refinement statistics for Cp1 at 1.12 Å

	Cp1 at 1.12 Å	
Data Collection Statistics		
Resolution range (Å)	38.91 – 1.12 (1.18-1.12)	
Wavelength (Å)	0.9537	
Space group	$P2_1$	
Unit cell constants	a = 72.8 Å	α = 90.00°
	b = 170.7 Å	β = 91.64°
	c = 87.5 Å	γ = 90.00°
Unique reflections	737,219 (86,732)*	
Completeness (%)	90.7 (73.1)*	
Redundancy	3.5 (3.4)*	
$I/\sigma(I)$	17.3 (3.2)	
R_{merge}	0.030 (0.317)*	
Refinement Statistics		
Protein residues	1951/1982	
Mean B value (Å^2)	11.6	
R_{work}	0.129	
R_{free}	0.151	
Ramachandran outliers	11 (0.59%)	
RMSD bond lengths (Å)	0.015	
RMSD bond angles (°)	1.80	

In the publication of the original Cp1 structure, two crystal forms, obtained from crystallization with magnesium chloride or cesium chloride (PDB ID 1MIO), were reported.[65] The unit cell dimensions of the structure presented here are similar to cesium chloride form; however, no cesium was used in the crystallization condition. Superposition of the secondary structure elements (1917/1951 residues) of 1MIO and the 1.12-Å structure gives a root mean square deviation of 0.152 Å.

III.C. Comparison to the Av1 structure

III.C.i. Insertion sequences

The shared sequence identity of Cp1 compared to Av1 is 37.7%. Superposition of the secondary structure elements (1738/1951 residues) of Av1 (PDB ID 3U7Q) and the 1.12-Å structure gives a root mean square deviation of 1.56 Å. The metalloclusters are identical, and the secondary structure elements are similar with two notable exceptions (Figure III-1): (1) an insertion sequence in the Cp1 α-subunit on the protein surface involving Cp1 residues α-Glu376–α-Gly428 and (2) a deletion in the Cp1 β-subunit on the protein surface involving Av1 residues β-Met1–β-Thr48.[21] Herein, these sequences are referred to as the Cp1 and Av1 insertion sequences, respectively.

The Cp1 insertion sequence consists of a flexible loop flanked with alpha helices; loop residues α-387–α-391 block the docking of the Fe protein when compared to Av1-Av2 complexes.[28,67] This is according to overlays with four different Av1-Av2 complexes (Figure III-2). These complexes were formed using additives to mimic nucleotide-free and nucleotide-bound conditions representing different conformations at various stages of electron transfer during substrate reduction.[28,67] Notably, Av1 and Cp2 form an inactive complex,[68,69] suggesting that there is something unique about the Cp1-Cp2 complex compared to the other nitrogenase

species, which likely involves the insertion sequence. Perhaps a different docking formation is adopted, or perhaps the loop flexes away from the protein in solution to open up the docking site. The latter is supported by the fact that there are only four polar contacts between residues in the loop portion of the insertion sequence and the rest of the protein.

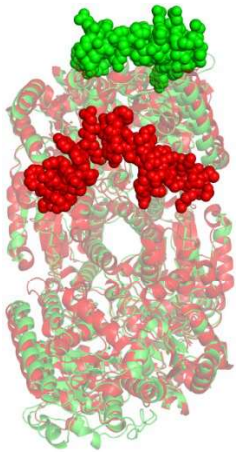

Figure III-1. Overlay of Cp1 (green) and Av1 (red, PDB ID 3U7Q) with insertion loops displayed as spheres. The insertion loops are shown in only one of the heterodimers.

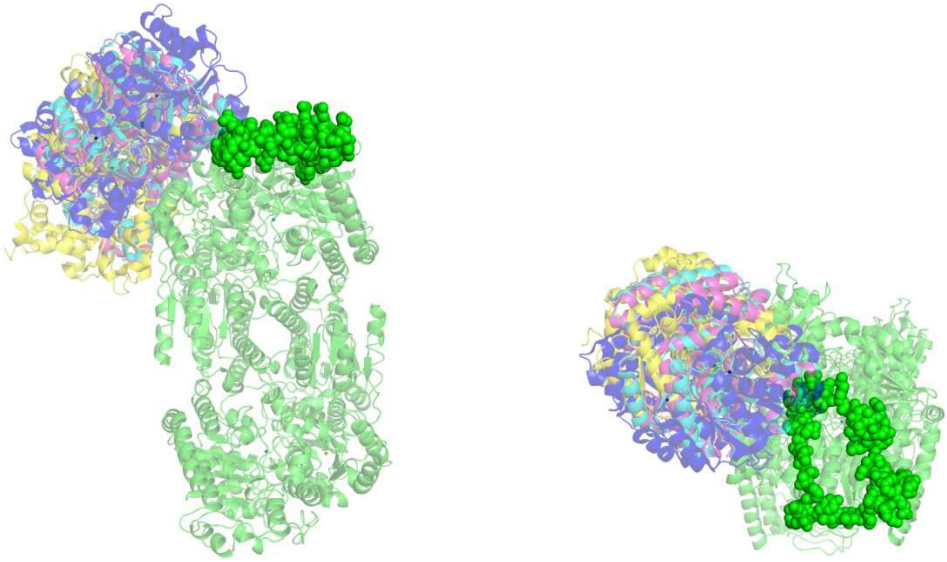

Figure III-2. Two orientations of overlays of Av2 (various colors) and Cp1 (green). The complexes include ADP·AlF_4^- stabilized Av1-Av2 (PDB ID 1M34, magenta), nucleotide-free Av1-Av2 (PDB ID 2AFH, yellow), MgAMPPCP-bound Av1-Av2 (PDB ID 2AFK, cyan), and MgADP-bound Av1-Av2 (PDB ID 2AFI, blue).[27,28] Av1 was used to create the superposition, but is hidden in the figure.

The Av1 insertion sequence initiates the β-subunit: the first quarter consists of a loop, followed by an alpha helix, another loop section, and another alpha helix. The Av1 insertion sequence partially covers opening of the interstitial water channel that connects the protein surface to the active site. This may impede access of small molecules to and from the active site. There are many polar contacts between the Av1 insertion sequence and the rest of the protein, which may indicate that the insertion sequence is not flexible.

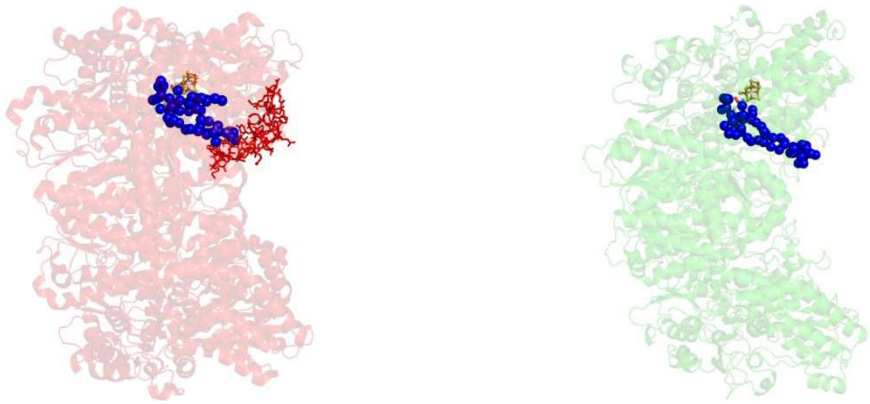

Figure III-3. (left) Av1 and (right) Cp1 with the water molecules of the interstitial channel shown in blue spheres. The residues of the Av1 insertion loops are displayed as sticks in the left figure. The Av1 insertion loop partially blocks the mouth of the interstitial channel. The FeMo-cofactor in both figures is shown with ball and stick and colored by element.

III.C.ii. Inter-subunit contacts

The contacts between the α, β, α', and β' subunits of Cp1 were determined using the program NCONT in the CCP4 suite (Table III-2).[58] A contact is defined as a distance of ≤3.5 Å between two atoms of different subunits. Contacts that are hydrogen bonds or electrostatic interactions are identified as salt bridges. There is a similar number of total contacts between all subunits in Av1 and Cp1, and most are salt bridges. The total number of salt bridges between all subunits is also similar, except in the case of the Cp1 β and β', which have about 50% more salt

bridges compared to other subunit interactions. The conservation of total contacts and salt bridges indicates that the interaction between subunits is not highly conserved.

Table III-2. Inter-subunit contacts in Av1 and Cp1

Subunits	Av1 β, β'	Cp1 β, β'	Av1 α, β	Cp1 α, β
Total number of contacts	58	59	58	59
Number of salt bridges	33	46	31	33
Conservation of total contacts in Av1 and Cp1	24 (41%)		29 (54%)	
Conservation of salt bridges in Av1 and Cp1	25 (63%)		17 (55%)	

III.C.iii. Conservation of tryptophan

The conservation of tryptophan residues was investigated since this amino acid is often involved in protein electron transfer reactions.[70] There are only six tryptophan residues in Cp1 (Figure III-4), compared to 18 in Av1 and 15 in Kp1. Of the six Cp1 tryptophan residues, four are conserved in Av1 and Kp1, including α-Trp223, α-Trp281, α-Trp512, and α-Trp519 (Table III-3). Only α-Trp84 resides near a cofactor; thus, this residue may have a role for in the substrate reduction mechanism. The five tryptophan residues in the α-subunit are all highly conserved.

Table III-3. Conservation of Cp1 tryptophan residues in groups I and II

	α-Trp84	α-Trp223	α-Trp281	α-Trp512	α-Trp519	β-Trp380
Conservation in group I (single variant mutant)	82% (Arg)	100%	100%	98% (Ile)	87%	0%
Conservation in group II (single variant mutant)	100%	72%	100%	94% (Phe)	89% (Phe)	67%
Overall conservation	87%	92%	100%	97%	87%	19%
Distance to FeMo-co (Å)	12	15	15	21	38	26
Distance to P-cluster (Å)	11	28	30	30	41	34

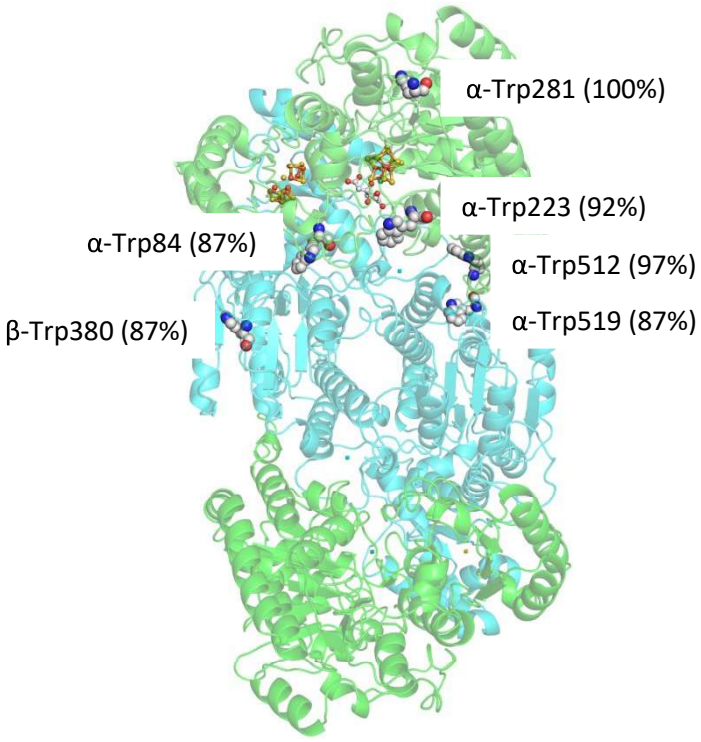

Figure III-4. Location of Cp1 Trp residues; their conservation in groups I and II are given in parentheses. The α subunits are shown in green and the β subunits are shown in cyan. The cofactors and the tryptophan residues are displayed with ball-and-stick and are colored by element.

III.C.iv. FeMo-cofactor insertion pathway

A pathway has been postulated for FeMo-cofactor insertion into the apo-MoFe protein.[71] This pathway was found in a structure of the Δ*nifB* protein, which lacks the FeMo-cofactor; the pathway is of sufficient width and is positively charged so as to accommodate the size and negative charge of the FeMo-cofactor. This pathway consists of three sections: (1) the lid-loop region (α-353–α-364), which may guide the FeMo-cofactor to the pathway, (2) the His-triad (α-His274, α-His442, and α-His451), which may provide binding site for the FeMo-cofactor during its journey, and (3) the switch/lock region (α-His442 and α-Trp444), which may secure the FeMo-cofactor in place by movement of residue side chains. Conservation of residues in the lid-loop, His-triad, and switch/lock regions are well conserved in group I (the Av1 homologs),

with a total of 88% conservation. The corresponding residues of the lid-loop, His-triad, and switch/lock regions in Cp1 are conserved in group II at 71%, suggesting that the FeMo-cofactor may have a different insertion pathway in Cp1 compared to Av1. Mutation studies as well as structural analysis of the Δ*nifB* Cp1 protein would be more conclusive.

III.C.v. Conservation of the contacts between the MoFe and Fe proteins

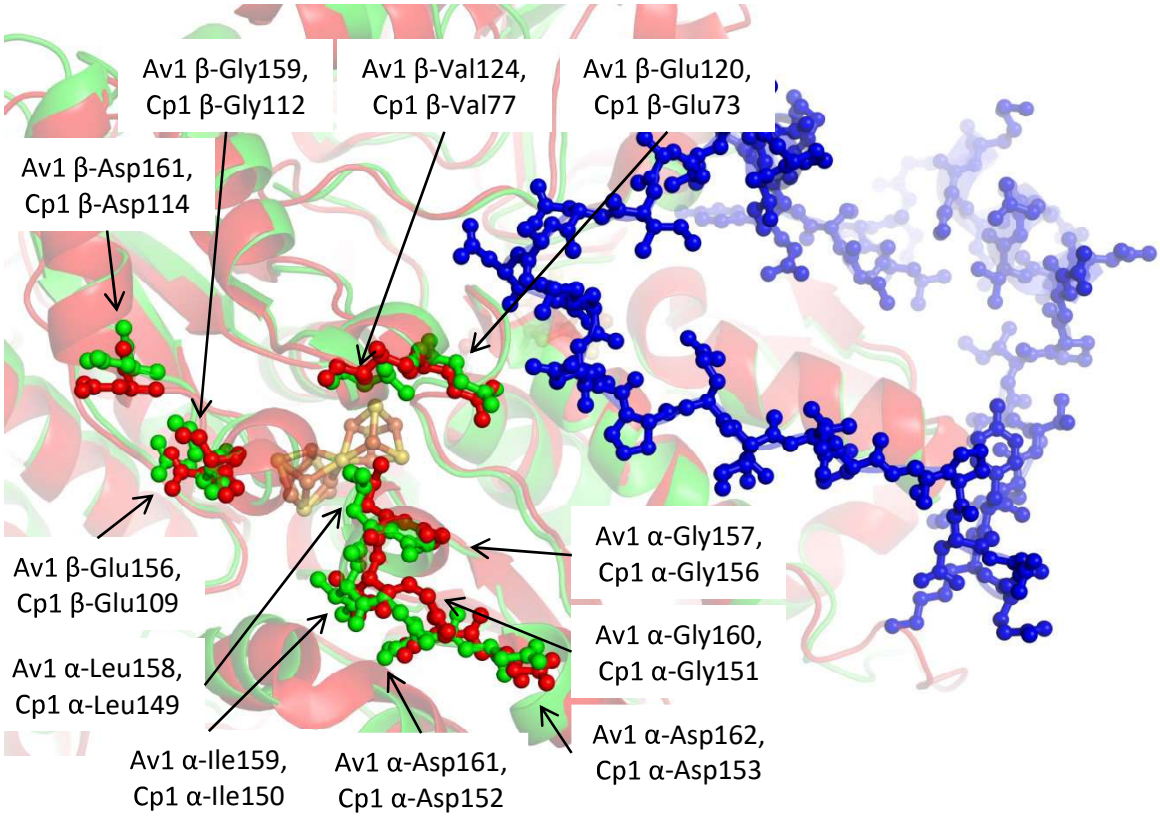

Figure III-5. Overlay of Av1 (red) and Cp1 (green). Of the 38 Av1 residues that have contact with Av2, 11 are conserved 100% among group I and II homologs. These residues are shown in ball-and-stick and are labeled. The P-cluster is shown in ball-and-stick and colored by element, and residues of the Cp1 insertion loop are shown in blue ball-and-sticks.

38 surface Av1 residues have contacts with Av2,[27,28] of which 15 are conserved 100% among group I homologs and may therefore serve in Fe protein docking. No Cp1-Cp2 structure has yet been reported. It is expected that the docking may have a different conformation due to

the Cp1 insertion sequence. Conservation of the Cp1 residues corresponding to the 18 Av1 residues with highly conserved contacts to Av2 was investigated. 11 of these 18 residues are conserved 100% in group II (Figure III-5). These residues are within close proximity of the P-cluster and are not blocked surface access by the Cp1 insertion loop. Because of this and the high conservation of these residues, they may be involved in the docking of Cp2 onto Cp1.

III.D. The interstitial atom of the FeMo-cofactor

Identification of the interstitial atom in the Av1 FeMo-cofactor as carbon was achieved in 2011 through a combination of X-ray crystallography, electron spin echo envelope modulation, and X-ray excitation spectroscopy.[22,72] Accurate electron density calculations from an X-ray crystal structure require atomic resolution due to Fourier series termination effects from the six iron atoms encasing the interstitial atom in a trigonal prism. This effect led to the masking of *all* electron density at the interstitial cavity for structures with resolutions worse than 1.5 Å and the incorrect identification of the interstitial atom as nitrogen in a 1.16 Å structure.[21,66,65,73–75]

Using the 1.08 Å Cp1 crystal structure, the electron density as a function of the radius from the atom center was calculated for all carbon, nitrogen, and oxygen atoms in the protein structure with a *B*-factor <30 Å^2 (Figure III-6). The electron density of the interstitial atom aligns best with the average carbon in the protein structure (Figure III-7). Although the interstitial atom of the FeMo-cofactor is likely electronically different from the average carbon in the protein scaffold, these methods were previously verified as reliable by spectroscopic techniques for use on structures at atomic resolution.[72]

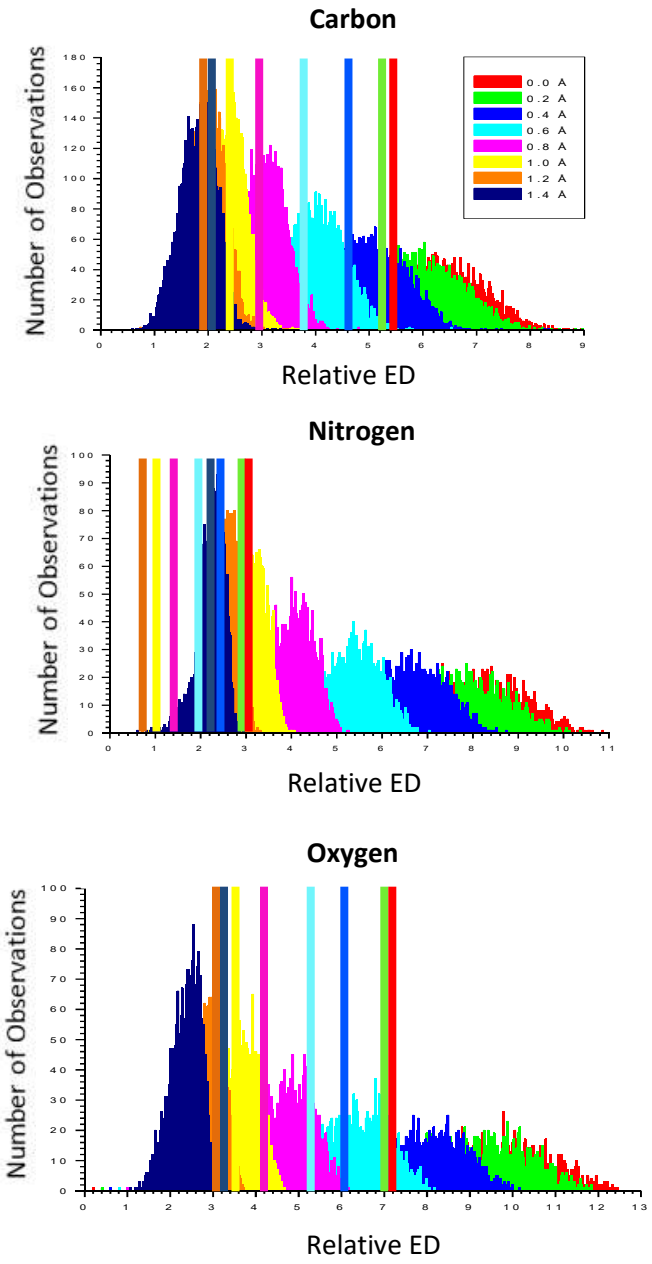

Figure III-6. Distribution plots of the electron density of all carbon, nitrogen, and oxygen atoms as a function of integration radius. The electron density of the interstitial atoms (solid lines) is overlaid on each plot. The overlay with the highest correlation is carbon. Two patterns are apparent from examination of the distribution plots. First, the distribution broadens as the integration radius decreases. This occurs because at larger integration radii, different distributions of the electrons in each electron cloud cause greater variations in the overall electron density. Second, the electron density decreases as the integration radius increases. Because the electron cloud is the most concentrated near the atom center, the average electron density at any given point in the electron cloud decreases at larger integration radii.

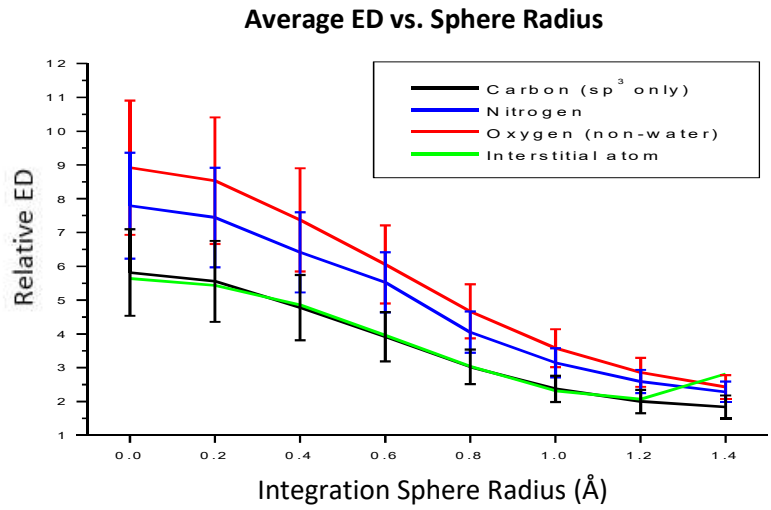

Figure III-7. Summary of results from Figure III-6 with Gaussian fitting. The error bars show one standard deviation from the mean electron density at each integration radius. The best correlation for the interstitial atom is carbon. The electron density of the interstitial atoms increases quite significantly at an integration radius 1.4 Å compared to other carbon atoms in the protein structure. This may result from incorporation of electron density of neighboring Fe atoms in the FeMo-cofactor, which are 2 Å from the interstitial carbon.

It was evident that there are different types of carbon and oxygen atoms in the protein structure from shoulders in the distribution plots of carbon and oxygen (Figure III-8). Further analysis showed that the right-hand shoulder in the carbon distributions is from sp^2 carbon atoms, which have greater electron density than sp^3 carbon atoms due to shorter bond lengths of double bonds compared to single bonds. The electron density of the interstitial atom correlates best with sp^3 carbon atoms compared to sp^2 carbon atoms. Although the interstitial carbon atom is coordinated to six iron atoms and exists as carbide (C^{4-}), the electron density distributions suggest that the iron atoms pull enough electron density away from the interstitial carbon such that it mimics the electron density of sp^3 carbons. Regarding the oxygen distributions, the left-hand shoulder is from oxygen atoms in water molecules (Figure III-8). The water oxygen atoms have less electron density than the protein backbone oxygen atoms

because the hydrogen atoms in a water molecule provide very little additional electron density compared to the carbon atoms in the protein scaffold.

From the X-ray crystallography data, the electron density at the atom center of each carbon, nitrogen, and oxygen atom was calculated as a function of *B*-factor and compared to that of the interstitial atoms (Figure III-9). Based on this comparison, the best fit for the interstitial atoms is carbon, as also concluded from electron density calculations and observed in Av1. This aligns with the observed minimal deviation in bond length (<0.09 Å) between all atoms in the cofactors (Table III-S1), which suggests that atomic identity is conserved in Av1 and Cp1.

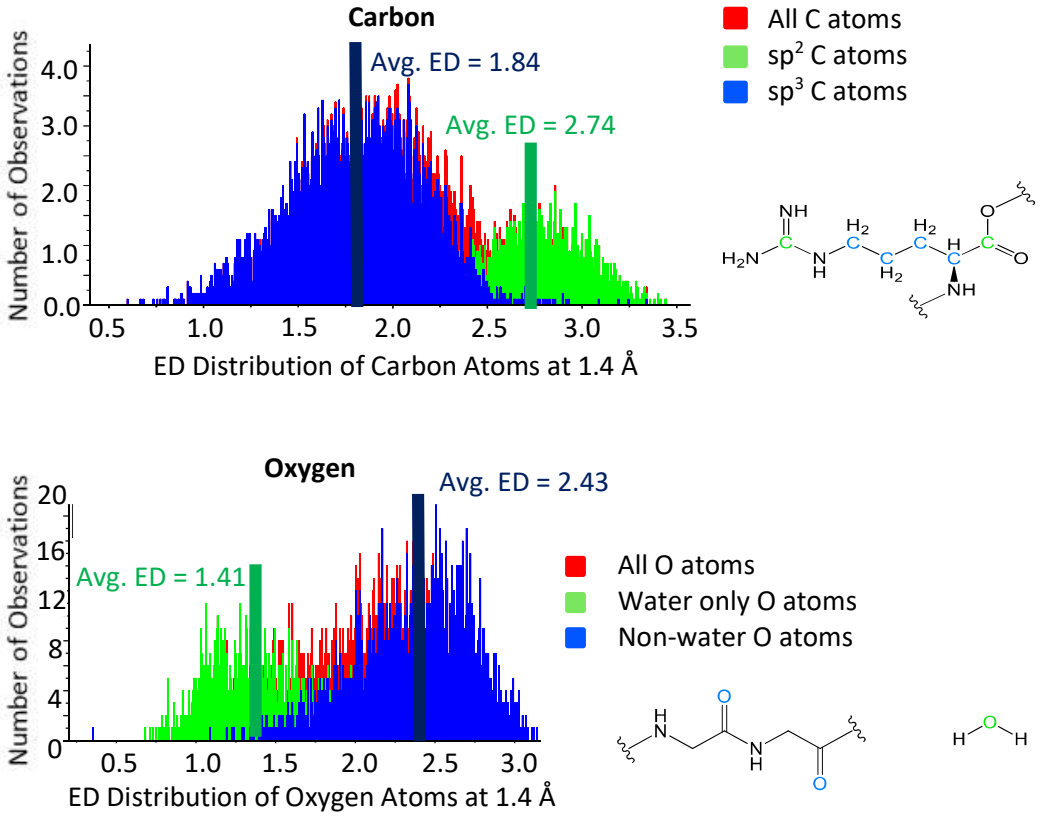

Figure III-8. Electron density distributions for carbon and oxygen at 1.4 Å show that different bonding environments lead to different electron densities.

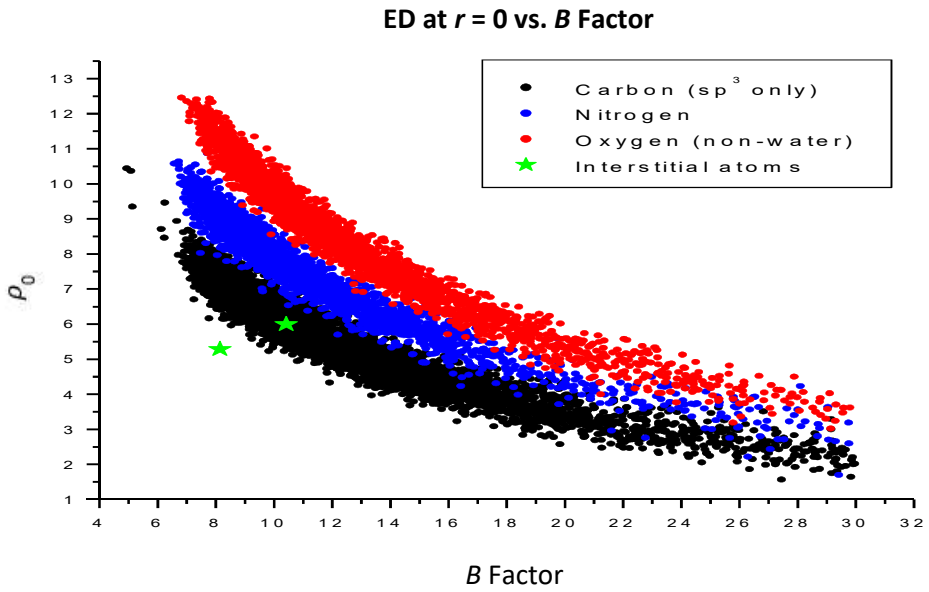

Figure III-9. Electron density of carbon, nitrogen, and oxygen atoms as a function of *B* factor.

III.F. The P-cluster

III.F.i. Comparing the reduced and oxidized states

As illustrated in Figure III-10, the P-cluster is stabilized by the following contacts in Av1: α-Cys154 to Fe1, α-Cys62 to Fe3, β-Cys95 to Fe2 and Fe8, α-Cys88 to Fe4, β-Cys70 to Fe7 (corresponding to Cp1 residues α-Cys145, α-Cys53, β-Cys48, α-Cys79, β-Cys23, respectively). In the open state of the P-cluster, Fe5 and Fe6 are stabilized by Av1 α-Cys88 (Cp1 α-Cys79) and Av1 β-Ser188 (Cp1 β-Ser141), respectively. In the closed state, Fe5 and Fe6 are stabilized by Av1 α-Cys88 (Cp1 α-Cys79) and Av1 β-Cys153 (Cp1 β-Cys106), respectively. The open and closed states of the P-cluster are the oxidized and dithionite-reduced forms, respectively.[75] X-ray crystal structures of Cp1 and Av1 typically show that the P-cluster is in the dithionite-reduced state or a mixed state. In a mixed state, Fe5 and Fe6 are modeled in both the closed and open conformations with a combined occupancy of 100%.

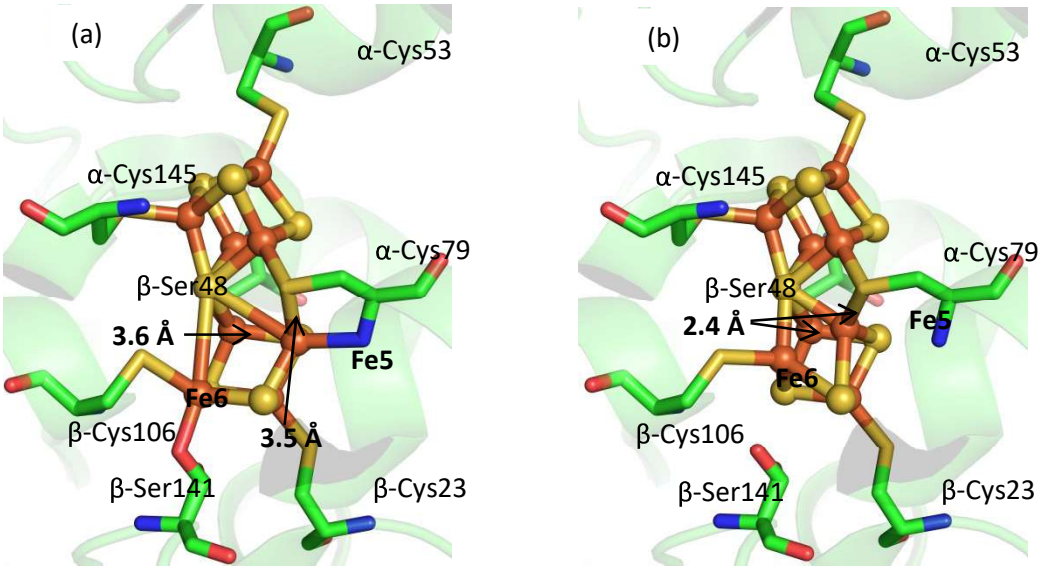

Figure III-10. The open (a) and closed (b) states of the P-cluster, corresponding to the putative oxidized and dithionite-reduced states, respectively. Fe5 and Fe6 are labeled as well as the bond length between these atoms and S1. The distance between S1 and Fe5,6 decreases from ~3.6 Å to 2.4 Å when going from the open to closed state. In both figures, the protein scaffold is shown in green cartoon and residues coordinated to the P-cluster are shown in sticks. The atoms of the P-cluster are represented with spheres and colored by element.

Residue β-Ser92 in Av1 may have a functional role in the MoFe protein, as deduced from its two alternate conformations in the reduced and oxidized Kp1 structures.[66] In the oxidized-state, the serine sidechain hydrogen bonds to a water molecule; in the reduced-state structure, the sidechain hydrogen bonds with S2A in the P-cluster. In the (dithionite-reduced) Cp1 structure presented here, the distance between Cp1 β-Ser45 and S2A is 2.9 Å. The dependence of this residue on the oxidation state of the cofactors and its strict conservation in groups I and II suggests that it could be involved in redox reactions and/or may provide structural support for the reduced-state P-cluster.

When the P-cluster is in the reduced state, Fe5 and Fe6 open up so as to form more hydrogen bonds between Fe6 and β-Ser188 in Av1 and β-Ser141 in Cp1. In group II, this serine is strictly conserved. In group I, however, β-Ser188 is conserved only 60%, and the only variant is

alanine. Although alanine is roughly the same size as serine, it is not capable of electrostatic interactions with the P-cluster. Interestingly, there are no nearby residues able to interact with Fe6 in the case of the Ser188Ala substitutions in Av1. This suggests that this serine may not be essential to the structure or function of nitrogenase.

III.G. Conclusions

This work showcases the first high resolution structure of a MoFe protein from group II, allowing detailed comparisons to be made between the most structurally divergent nitrogenase MoFe protein groups known. Notably, the interstitial carbon atom in the FeMo-cofactor in conserved, from which we can conclude that the structure of the cofactors (including the P-cluster) are identical in groups I and II. There are, however, differences in the structure of the protein scaffold that suggest alternative Fe protein docking, substrate and product pathways, FeMo-cofactor insertion pathways, and cofactor environment. These differences and their potential impact on the mechanism of substrate reduction will be better understood by characterizing Av1 and Cp1 under turnover conditions as well as Cp1-Cp2 complexes.

III.H. Experimental (see publication for further detail)[64]

III.H.i. Protein purification and crystallization

Purification of Cp1 was performed as previously described.[21] Cp1 was crystallized using the sitting-drop vapor diffusion method with a reservoir solution containing 0.2 M lithium citrate and 20% (w/v) PEG 3350 at room temperature in an anaerobic chamber. The resulting crystals were soaked in reservoir solution containing 10% 2-methyl-2,4-pentanediol (MPD) and 5 mM sodium dithionite for 15 min before flash-freezing in liquid nitrogen.

III.H.ii. Data collection and processing

X-ray diffraction data were collected on beam line 12-2 at the Stanford Synchrotron Radiation Lightsource (SSRL), with a Pilatus 6M pixel array detector. The 1.12 Å-resolution diffraction data set was collected at 14,000 eV with an oscillation angle of 0.15°. The data were integrated with the XDS program package.[57] The model was built manually in COOT using the electron density map from experimental phasing,[21,76] and the structure was refined with REFMAC5.[60] Structure validation analysis was done using MolProbity v4.02.[77] Intermolecular contacts were analyzed using the CCP4 program CONTACT.[58] Figures were prepared in PyMOL.[63]

Electron density analyses was carried out using proprietary software. First, all atoms of interest were selected from the PDB file, which include those with *B*-factor <30 $Å^2$ and a correlation factor of 1. The electron density map was then divided into a 400 x 600 x 400 grid, yielding about 9.6 x 10^7 cubes, each with dimensions of 0.182 x 0.284 x 0.219 Å. Due to the small size of each cube compared to the size of an atom, it is assumed that each cube has uniform electron density. The masked electron density distribution file was then overlaid onto the PDB file. The program calculated the electron density of each atom at a given radius from the atom center by averaging the electron density of each box contained in the given radius. The electron density was calculated for each atom from the atom center (0.0 Å) to 1.4 Å with 0.2 Å intervals.

III.H.iii. Protein Data Bank accession numbers

Atomic coordinates and structure factors for the 1.08 Å structure were deposited in the Protein Data Bank with ID 4WES.

III.I. Acknowledgments

The work was supported by NIH grant GM45162 to D.C.R., and the National Sciences and Engineering Research Council of Canada and Caltech Center for Environmental Microbial Interactions fellowships to L.M.Z. We thank the staff at beam line 12–2, Stanford Synchrotron Radiation Lightsource (SSRL) for their assistance. We acknowledge the Gordon and Betty Moore Foundation, the Beckman Institute, and the Sanofi–Aventis Bioengineering Research Program at Caltech for their generous support of the Caltech Molecular Observatory.

III.J. Supporting information

Table III-S1. Comparison of Bond Lengths in the FeMo-cofactor and P-cluster of the Atomic Resolution structures of Av1 (PDB ID 3U7Q) and Cp1[22]

Bond	3U7Q	1.12 Å Cp1	Difference
FeMo-cofactor			
FE1-S1A	2.31	2.29	0.02
FE1-S2A	2.27	2.31	0.04
FE1-S4A	2.29	2.30	0.005
S1A-FE2	2.26	2.28	0.02
S1A-FE4	2.29	2.28	0.015
S2A-FE2	2.25	2.30	0.045
S2A-FE3	2.28	2.28	0.005
S4A-FE4	2.29	2.29	0.005
S4A-FE3	2.25	2.29	0.035
FE2-S2B	2.21	2.24	0.03
FE2-CX	2.01	2.02	0.01
FE3-S5A	2.23	2.23	0
FE3-CX	1.99	2.00	0.01
FE4-S3A	2.24	2.24	0.005
FE4-CX	2.00	1.97	0.03
FE5-S3A	2.26	2.20	0.06
FE5-CX	2.01	1.98	0.03
FE5-S1B	2.27	2.22	0.05
FE5-S4B	2.26	2.25	0.01
FE6-S2B	2.18	2.23	0.05
FE6-CX	2.02	2.03	0.015

FE6-S3B	2.22	2.25	0.025
FE6-S1B	2.24	2.25	0.01
FE7-S5A	2.21	2.23	0.015
FE7-CX	1.99	2.01	0.02
FE7-S4B	2.22	2.24	0.02
FE7-S3B	2.25	2.23	0.02
S1B-MO1	2.36	2.35	0.005
S3B-MO1	2.37	2.35	0.02
S4B-MO1	2.35	2.38	0.03
P-Cluster			
FE3-S2A	2.29	2.33	0.04
FE3-S3A	2.32	2.35	0.03
FE3-S4A	2.26	2.30	0.04
S2A-FE1	2.31	2.35	0.04
S2A-FE2	2.30	2.31	0.01
S3A-FE4	2.30	2.33	0.03
S3A-FE1	2.31	2.34	0.025
S4A-FE2	2.28	2.32	0.035
S4A-FE4	2.29	2.29	0
FE1-S1	2.39	2.38	0.01
FE2-S1	2.48	2.48	0.005
FE4-S1	2.38	2.39	0.01
S1-FE5,B	2.60	2.54	0.065
S1-FE5,A	3.81	3.72	0.085
S1-FE6,B	2.56	2.53	0.035
S1-FE6,A	3.86	3.80	0.065
S1-FE8	2.36	2.39	0.03
FE5,A-S4B	2.31	2.34	0.025
FE5,B-S4B	2.21	2.25	0.04
FE5,A-S2B	2.27	2.22	0.05
FE5,B-S2B	2.45	2.47	0.02
FE6,A-S2B	2.33	2.35	0.015
FE6,B-S2B	2.57	2.52	0.045
FE6,A-S3B	2.36	2.34	0.015
FE6,B-S3B	2.32	2.33	0.01
FE8-S3B	2.28	2.28	0.005
FE8-S4B	2.32	2.33	0.005
S2B-FE7	2.32	2.32	0
S3B-FE7	2.32	2.33	0.005
S4B-FE7	2.29	2.32	0.03